Time-division superconducting quantum interference device multiplexer for transition-edge sensors

Piet A. J. de Korte,[a] Joern Beyer,[b] Steve Deiker, Gene C. Hilton, Kent D. Irwin,[c] Mike MacIntosh,[d] Sae Woo Nam, Carl D. Reintsema, and Leila R. Vale
National Institute of Standards and Technology, Mail Stop 814.03, 325 Broadway, Boulder, Colorado 80303

Martin E. Huber
Department of Physics, University of Colorado at Denver, Denver, Colorado 80217-3364

(Received 16 July 2002; accepted 25 May 2003)

We report on the design and performance of our second-generation 32-channel time-division multiplexer developed for the readout of large-format arrays of superconducting transition-edge sensors. We present design issues and measurement results on its gain, bandwidth, noise, and cross talk. In particular, we discuss noise performance at low frequency, important for long uninterrupted submillimeter/far-infrared observations, and present a scheme for mitigation of low-frequency noise. Also, results are presented on the decoupling of the input circuit from the first-stage feedback signal by means of a balanced superconducting quantum interference device pair. Finally, the first results of multiplexing several input channels in a switched, digital flux-lock loop are shown. © *2003 American Institute of Physics.* [DOI: 10.1063/1.1593809]

I. INTRODUCTION

The excellent performance of optical-to-x-ray microcalorimeters and far-infrared-to-submillimeter bolometers, making use of superconducting-to-normal phase-transition thermometers, generally called transition-edge sensors (TES), has led to demands for large arrays for applications as diverse as materials analysis and astronomy. The low noise, low power, and low input impedance of superconducting quantum interference devices (SQUIDs) make them the preamplifier of choice for TES devices. Due to the constraints on wiring and circuit complexity, multiplexed readout schemes are required to instrument large-format arrays. Both time-division multiplexing (TDM) (Ref. 1) and frequency-division multiplexing (FDM) (Ref. 2) are presently under development. The tradeoffs between those two approaches are discussed extensively elsewhere.[3,4] Here, we describe the development of a TDM circuit.

The TDM performance of a TES sensor array is governed by several criteria, discussed in more detail elsewhere.[1,3] Nyquist's criterion for multiplexing many pixels with fast signals, as would occur in an optical or x-ray TES microcalorimeter array, asks for high sample rate and large system bandwidth. Multiplexing N channels increases the multiplexer (MUX) noise bandwidth, so the MUX noise level has to be $\sqrt{N}$ times smaller than for readout electronics of a single pixel to match the noise levels at the output. This so-called multiplex disadvantage requires a low input noise level for the MUX. The strongest constraint is set by the slew rate and dynamic range requirements for TES x-ray microcalorimeters as developed, for example, for NASA's Constellation X mission. This mission requires a combination of low input noise, high bandwidth and operation in flux-lock-loop (FLL) mode. In contrast, the observation of submillimeter/infrared radiation from the sky with a TES bolometer array requires very low low-frequency noise, thereby extending the period of uninterrupted observation. Most of these criteria will be addressed in this article.

II. MULTIPLEXER DESIGN

The design of a second-generation 32-channel MUX, the subject of this article, builds upon the experience accumulated with an earlier eight-channel device[1,5] that used a different circuit architecture. Our first-generation eight-channel TDM has now been used in a submillimeter instrument, FIBRE, recently tested at the Caltech Submillimeter Observatory.[6] Although the first-generation design worked satisfactorily, it suffered from limitations in scalability.[7]

The second-generation 32-channel multiplexer chip represents one column of a $32\times N$ array readout. Its design is shown in Fig. 1. Most of the symbols used throughout this article are defined in this design section and Fig. 1. The abbreviations L and M are reserved for self-inductance and mutual inductance, respectively. The second-generation MUX consists of two stages fabricated on one silicon chip and an off-chip third stage. This arrangement allows for operation of the first two stages near the TES at base temperature and the third stage at 4 K. The first stage contains 32 input SQUIDs (SQ1) including input coils (L_{IN1}), address resistors (R_{ADDRESS}), output transformers (TR), and a common feedback (FB1) line. The second stage includes a transformer loop (TL) common to the 32 input SQUIDs, which are coupled to that loop by means of the output transformers.

[a]On leave from the Space Research Organization Netherlands, Sorbonnelaan 2, 3584 CA Utrecht, The Netherlands.
[b]On leave from the Physikalische Technische Bundesanstalt, Berlin, Germany.
[c]Electronic mail: irwin@boulder.nist.gov
[d]Also at: Astronomy Technology Center, Edinburgh, UK.

 © 2003 American Institute of Physics

Downloaded 14 Oct 2003 to 142.103.234.76. Redistribution subject to AIP license or copyright, see http://ojps.aip.org/rsio/rsicr.jsp

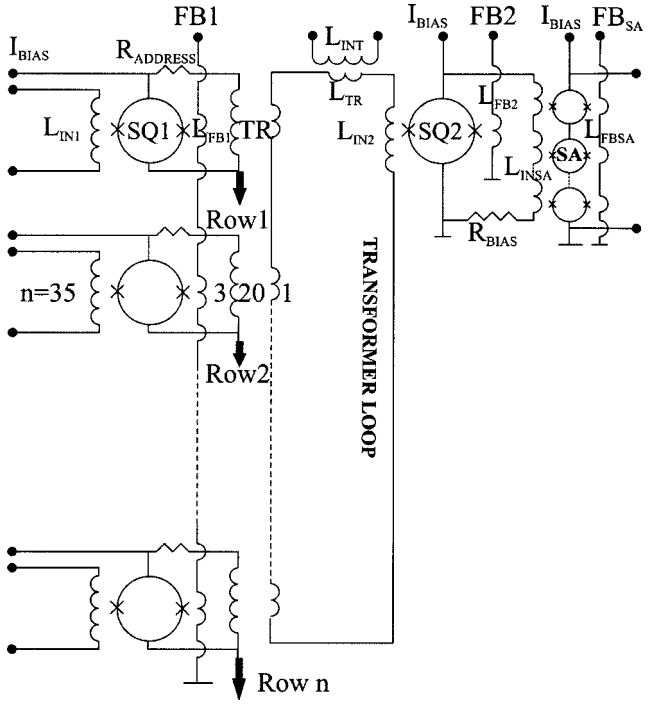

FIG. 1. MUX architecture. Only one column is shown. An address *current* switches on one row of first-stage series-connected SQUIDs at a time. An address resistor, $R_A = 1\ \Omega$, shunts each first-stage SQUID. The current through the address resistor arm runs also through a transformer coil, coupling the signal to a transformer loop, common to all first-stage SQUIDs in one column. The transformer loop is coupled to a second-stage SQUID by its input coil. Each second stage SQUID is voltage-biased, $R_{BIAS} = 90\ m\Omega$, and its output current is fed into the input coil of a current-biased series-array SQUID capable of carrying the voltage signal to room-temperature low-noise electronics. The series-array SQUID is not a part of the MUX-chip.

The TL is coupled to the second-stage SQUID (SQ2). A third stage series-array SQUID (SA), which is not part of the MUX chip, buffers the signal to the room-temperature electronics.

We have developed a series-address multiplexer architecture. To facilitate comprehension of this scheme, a two-dimensional schematic is shown in Fig. 2. In this approach, address currents ($I_{ADDRESS}$) are applied sequentially to turn on one row at a time. In the ''on'' row the SQ1s, each shunted with a resistor $R_{ADDRESS}$ of 1 Ω, are connected in series. The increase of the bias resistor $R_{ADDRESS}$ above 100 mΩ, typically used to voltage bias SQUIDs, results in improvements of the first-stage power consumption, reduces the Johnson current–noise contribution of the bias resistor, and improves the switch-off time constant of the first stage at the expense of a reduction of the first-stage gain. The output current of the first stage is inductively coupled to a common transformer loop by means of an output transformer in the bias-resistor arm of the first-stage circuitry. This arm is chosen since it has a lower dc current than does the SQUID arm. The transformer design is a tradeoff between first-stage gain and signal bandwidth.

The transformer loop is a closed stripline containing 32 secondary transformer coils and one input coil to the second-stage SQUID. To optimize the signal-to-noise ratio of the TL the total self-inductance of the secondary transformer coils $33L_{TR}$ is designed to equal the self-inductance L_{IN2} of the second-stage SQUID input coil. One of the input transformers is not coupled to a first-stage SQUID and can be used with an external current source for system testing. The second-stage SQUID is voltage biased with $R_{BIAS} = 90\ m\Omega$. This SQUID has a coil (FB2) coupled to it with a wiring option for two, four, or eight turns that is used to set a dc flux bias offset for the second-stage SQUID. In order to optimize the bandwidth of the second-stage bias circuit, a one-turn input coil series-array SQUID with a small inductance $L_{INSA} \approx 74\ nH$ is used. The series-array SQUID, which is not a part of the MUX chip, is current biased, and the feedback coil with inductance L_{FBSA} is used to set a dc flux bias offset.

SQ2 could also be a series-array SQUID, allowing direct

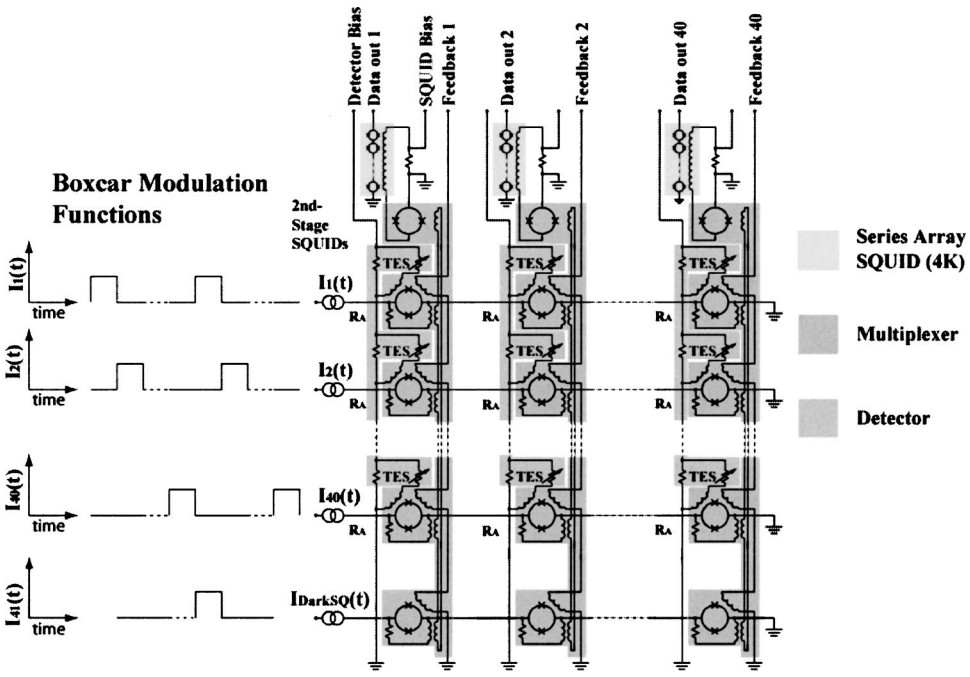

FIG. 2. Two-dimensional schematic of the MUX. The series connections of the SQ1 address lines, between the various columns, are shown as well as the dark SQUID for reduction of low-frequency noise.

Downloaded 14 Oct 2003 to 142.103.234.76. Redistribution subject to AIP license or copyright, see http://ojps.aip.org/rsio/rsicr.jsp

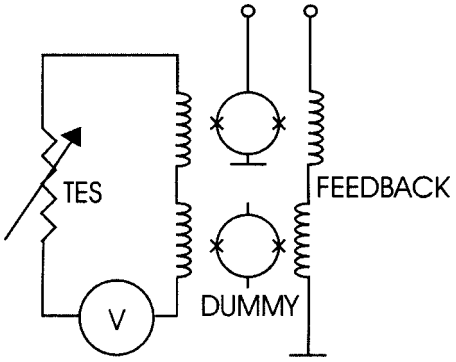

FIG. 3. Balanced SQUID-pair is designed to eliminate coupling between the common feedback line per column and the first-stage SQUID input circuits. The double feedback circuit has two coils, wound in opposite directions, thereby canceling the action of the feedback line on the input. Only one of the SQUIDs will be switched on-and-off during multiplexing. A dummy SQUID is implemented to match all inductances as closely as possible.

coupling to room-temperature electronics. This arrangement would result in a simplified two-stage MUX. However, our existing series-array SQUIDs dissipates up to 1 μW when optimally biased. This power may be too high to place at the base temperature of some cryostats. The second-stage SQUID can also be eliminated by carrying the superconducting transformer loop all the way to the series-array SQUID at 4 K. We have chosen the more complex three-stage design because it circumvents wiring, EMI, power dissipation, and shielding issues.

Another design issue is the coupling between the common first-stage feedback coil and the SQ1 input coil. When a feedback current is applied to flux lock the on SQUID, currents are induced in the input coils and consequently in the bias circuits of all the other detectors in that column. Since the currents induced in the detector bias circuits have a finite decay time, these induced currents result in cross talk between each on-channel and all the off-channels in one column (see Sec. IV E). In this second-generation design, this coupling is reduced by connecting the TES to the input coils of two input SQUIDs with oppositely wound feedback coils as shown in Fig. 3. Only one SQUID of the pair is turned on. A dummy SQUID structure is used for coupling of the second counterwound coil in order to match the mutual inductances as closely as possible.

III. MULTIPLEXER MANUFACTURING AND EXPERIMENTAL SETUP

The MUX chip has been made using a standard process for dc SQUID fabrication at NIST.[8] Typical performance figures for those SQUIDs are reported elsewhere.[9,10] In brief, we use Nb/AlO_x/Nb trilayer Josephson junctions, PdAu resistors, SiO_2 interlayers, and Nb wiring. The typical inductance of a single SQUID is $L_{SQ} \approx 18$ pH, the maximum critical current $2I_C = 100\,\mu$A, and the resistance of the shunt resistors is $R_{sh} = 1\,\Omega$. Figure 4 is a photograph of part of the 32-channel multiplexer chip.

Most of the measurements reported in this article were performed using a dip probe in a 4 K helium dewar. The MUX chip is clamped and bonded onto a PC board, which is

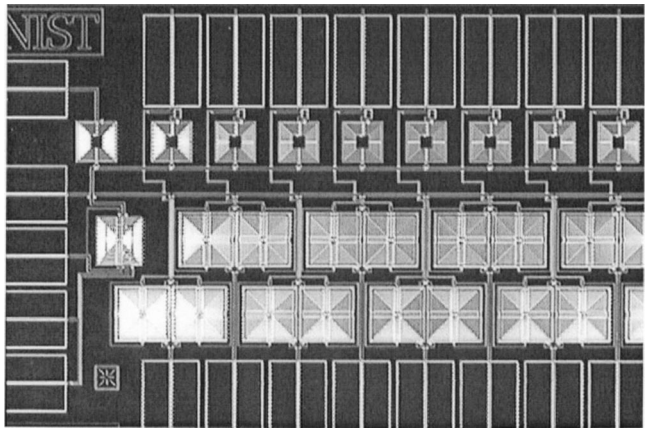

FIG. 4. Micrograph of part of the 32-channel MUX. The top row of coils are the transformers, coupling signals from the first-stage SQUIDs into the common transformer loop. The second and third row contains first-stage input SQUIDs, each channel consisting of a pair. The coil on the far left of the middle row is the second-stage SQUID, while the coil directly above it is the extra transformer. The pitch between each successive first-stage SQUID pair, alternatively on the second and third row, is 550 μm.

attached at the end of the probe. The bias and signal connections to this PC board are made by means of flexible cables to room temperature. Each has eight microstrip lines. A high permeability metal cylinder magnetically shields the PC board and MUX chip. The third-stage series-array SQUID is shielded by its own high permeability metal and superconducting shield.

IV. PERFORMANCE DATA AND INTERPRETATION

A. Dc parameters

The SQUIDs used have a flux-focusing washer electrically isolated from the SQUID. Although this design reduces the coupling efficiency to the device it tends to result in less resonance.[9] Resonance damping is also obtained via intracoil damping resistors R_{ic},[10] which are not shown in Fig. 1. In order to increase the chance for nonresonant operation of this MUX chip the intracoil damping resistances for the first production batch were chosen conservatively, i.e., $R_{ic} = 30\,\text{m}\Omega/\text{turn}$. Some measured and calculated parameters for the SQUIDs on this multiplexer chip are given in Table I. The calculated values are shown within parentheses.

Although SQ1 is almost identical to SQ2, differences in the maximum current modulation ΔI_{max}, the transfer coefficient $I_\Phi = (\partial I/\partial \Phi)$, and the dynamic resistance R_{DYN} at the operation point, arise due to different bias conditions. Setting the bias current for the maximum current modulation ΔI_{max} and the flux bias for the middle of the $I-\Phi$ curve, we get the range of I_Φ and R_{DYN} given in Table I. The two values for I_Φ originate from a difference in the positive and negative slopes of the measured $I-\Phi$ curves. The total power consumption of the first stage at the optimum bias point for SQ1 is 2.0 nW for SQ1 itself and 0.4 nW for $R_{ADDRESS}$. For the second stage, the breakdown is 0.9 nW for SQ2 itself and 0.7 nW for R_{BIAS}. The total power consumption per column of 4 nW is close to a typical TES power consumption for 32 pixels of 0.8 nW. The measured mutual inductances are consistent with 9 pH per turn, so this value is also used to cal-

Downloaded 14 Oct 2003 to 142.103.234.76. Redistribution subject to AIP license or copyright, see http://ojps.aip.org/rsio/rsicr.jsp

TABLE I. Dc parameters of SQ1, SQ2, TR, and SA.

	$2I_C$ (μA)	ΔI_{max} (μA)	I_Φ ($\mu A/\Phi_0$)	R_{DYN} (Ω)	Power (nW)	M_{IN}^{-1} ($\mu A/\Phi_0$)	M_{FB}^{-1} ($\mu A/\Phi_0$)	L_{IN} (nH)
SQ1	102	34	94 or 118	1.4–1.6	2.4	6.5	75.7	130 (67)
SQ2	117	60	116 or 182	3.0–6.0	1.6	(15.3)	44.1	(8.0)
TR						(0.59)		74 (73)
SA				153	≈1000	(213.7)	213.7	74

culate M_{IN2}. The value measured for M_{FB2} is smaller, i.e., 5.9 pH per turn, due to screening by the transformer loop, as explained below. For the self-inductances of the SQUID input coils, only the value for L_{IN1} of SQ1 can be measured directly. The other values are calculated on the basis of self-inductances measured for 19- and 50-turn input coils on a similar SQUID. Those data can be fitted using a washer inductance of 26.7 pH and a stray inductance of 0.22 nH/mm, as expected for the stripline coil.[11] The large difference between the washer inductance and mutual inductance per turn is due to the floating washer geometry. The large discrepancy between the measured and calculated inductance L_{IN1} for the double first-stage SQUID 35-turn input coil is assumed to originate from stray inductances off-chip.

The signals from the multiplexed first-stage SQUIDs are coupled to the transformer loop by means of a 20:1 transformer. By applying an input current ΔI_{INT} to the spare input transformer and measuring the flux change $\Delta\Phi_{SQ2}$, we measured a transfer $\Delta I_{INT}/\Delta\Phi_{SQ2}=105\,\mu A/\Phi_0$. Simple considerations lead to

$$\Delta I_{INT}/\Delta\Phi_{SQ2}=L_{TL}/(M_{INT}M_{IN2}), \tag{1}$$

where L_{TL} is the inductance of the transformer loop, M_{INT} is the mutual inductance of the transformer, and M_{IN2} is the mutual inductance between SQ2 and its input coil. Since SQ2 is very similar to SQ1 and other NIST SQUIDs we calculate M_{IN2}^{-1} to be $15.3\,\mu A/\Phi_0$, so that $L_{TL}/M_{INT}=6.9$. The transformer has a square hole of size $d=110\,\mu$m, an input coil with $n=20$ turns, and an output coil of $n=1$ turn. Assuming perfect coupling, M_{INT} is calculated to be 3.5 nH,[11] which results in a value for $L_{TL}=23.9$ nH. Another approach to obtain L_{TL} is to add the estimated inductances for all the elements, i.e., 8 nH for L_{IN2} (Table I), and 0.47 nH for each of the $33\,L_{TR}$, each consisting of a coupled inductance $L_{TRC}=0.17$ nH and a stray inductance $L_{TRSTRAY}=0.3$ nH. The self-inductance of the stripline common transformer loop itself can be neglected, given its width of 20 μm. So the total calculated inductance $L_{TL}=L_{IN2}+33L_{TR}=23.5$ nH is consistent with the measurement of $\Delta I_{INT}/\Delta\Phi_{SQ2}$. The data show that $L_{IN2}\neq 33L_{TR}$, so there remains some room for optimization of the system signal-to-noise ratio and bandwidth.

The calculated value of $L_{INT}=73$ nH is consistent with direct measurement.

B. Frequency response and bandwidth

The frequency response of the MUX can be described by a multiplication of the various poles in the system. The first stage contains two poles. One is due to the intracoil damping resistors on the input coil L_{IN1}. Using the calculated inductance of 67 nH for the SQUID pair, this pole frequency equals 4.4 MHz. The other is due to the bias circuit of the first-stage SQUID i.e., $[(R_{DYN}+R_{ADDRESS})//R_{ICDINT}]/2\pi L_{INT}$, with $R_{ICDINT}=10\,\Omega$, the intracoil damping resistance on the transformer coil. Use of Table I gives a pole frequency at 4.2–4.4 MHz.

The flux generated in the second-stage SQUID by a first-stage output current I_{OUT}, coupled by means of the transformer, is given by

$$\frac{\partial\Phi_{SQ2}}{\partial I_{OUT}}(\omega)=\frac{M_{INT}M_{IN2}}{L_{TL}(\omega)}. \tag{2}$$

This relation is in accordance with relation (1), which contains the low-frequency value $L_{TL}(0)$ for the transformer loop inductance. If one of the first-stage SQUIDs is on, and neglecting the intracoil damping resistors on the transformers, we have

$$L_{TL}(\omega)=[L_{IN2}+33(L_{TRSTRAY}+L_{TRC})]-31L_{TRC}\frac{(\omega/\omega_1)^2k^2}{1+(\omega/\omega_1)^2}. \tag{3}$$

The self-inductance L_{TL} contains not only L_{IN2}, L_{TRC}, and $L_{TRSTRAY}$, the first term on the right side of the equation, but also the influence of screening by 31 first-stage off-SQUID bias circuits, containing $L_{INT}=74$ nH and $R_{ADDRESS}=1\,\Omega$, where $\omega_1=R_{ADDRESS}/L_{INT}$ and k equals the coupling constant of the transformer coils. At frequencies well above $\omega_1/2\pi=2.15$ MHz, the inductance of the transformer loop should decrease by $31L_{TRC}=5.3$ nH. This results in an increase of the high-frequency transformer signal transfer. The second stage contains two more poles. The first is due to the intracoil damping resistors on the input and feedback coils of SQ2. Assuming perfect coupling between both coils we calculate a pole frequency of 5.3 MHz. The other pole is due to the bias circuit of SQ2 and has a frequency of $[(R_{DYN}+R_{BIAS})//R_{ICDSA}]/2\pi L_{INSA}$. With the values in Table I and an intracoil damping resistor $R_{ICDSA}=50\,\Omega$ on the input coil of the series-array SQUID the pole frequency ranges between 6.3 and 11.7 MHz.

The measurement of the frequency-response function of the MUX using the feedback coil of the second SQUID as an input is another way to characterize screening by the transformer loop. In this case, the frequency response decreases for higher frequencies as shown by

$$\frac{\partial\Phi_{SQ2}}{\partial I_{FB}}(\omega)=M_{FB2}\left[1-\frac{k_cL_{IN2}}{L_{TL}(\omega)}\right], \tag{4}$$

Downloaded 14 Oct 2003 to 142.103.234.76. Redistribution subject to AIP license or copyright, see http://ojps.aip.org/rsio/rsicr.jsp

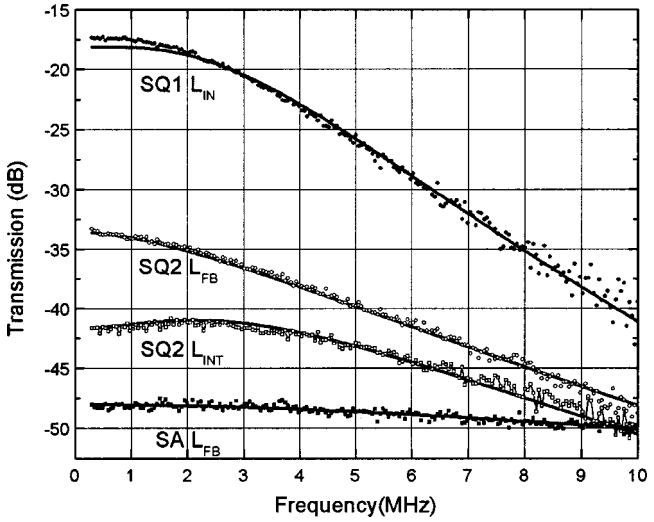

FIG. 5. Frequency response for the various MUX stages. All measurements have been taken in open loop using a network analyzer. The parameters used for the various fits are described in detail in the text.

where k_c is the coupling constant between input and feedback coils of SQ2, and is expected to be close to 1.0. $L_{\mathrm{TL}}(\omega)$ is the impedance of the transformer loop given by relation (3). However, since this frequency response is measured with all first-stage SQUIDs turned off, the last term in Eq. (3) should have a prefactor of 32 instead of 31.

The frequency response for various stages of the MUX is measured with a network analyzer. For these measurements, the output of the series-array SQUID is ac coupled to the network analyzer with 50 Ω input impedance. The data and respective fits are shown in Fig. 5, while the calculated and fitted pole frequencies are summarized in Table II.

The frequency response of the series-array SQUID can be fit as a one-pole low-pass filter with a corner frequency of 13 MHz. This roll-off is consistent with an RC–time constant caused by the dynamic resistance of the SQUID array $R_{\mathrm{DYN}} \approx 120-150\,\Omega$ and the measured capacitance of about 100 pF of the wiring from 4 K to room temperature. The intrinsic bandwidth of the SQUID array is at least 100 MHz.[9]

The frequency response of the second MUX stage has been measured at two different inputs, i.e., the feedback coil of SQ2 and the additional transformer input into the transformer loop. The spectra of those two frequency responses are distinctly different. The transfer function for the SQ2 feedback coil input decreases for higher frequencies, while the one measured for the input at the transformer loop increases with higher frequencies (see Fig. 5). Fitting the second-stage data we find that the amplitude difference between the two different spectra is consistent with the measured dc values in Table I. In order to obtain good fits to the shapes of both frequency response curves, 9 nH has to be screened out of the transformer loop, instead of the expected 5.7 nH due to the screening action by the 32 first-stage off-SQUIDs. The pole frequency fitted for the screening, 2.2 MHz, agrees with the predictions. To fit the above data, the two second-stage poles discussed above also have to be fitted. The fits result in a pole at 5.3 and 8 MHz, in agreement with those calculated.

The frequency-response fit for a signal input at the input coil of the first-stage SQUID uses the SQ2 response model for input at the transformer as described above, and multiplies this with two additional poles at 4.4 and 5.6 MHz. The poles are calculated to be at 4.4 and 4.2–4.4 MHz. Therefore, the pole due to first-stage intracoil damping is at a frequency equal to or larger than 4.4 MHz, which means that (1) the calculated value for L_{IN1}, 67 nH, is correct, and (2) the high measured inductance for L_{IN1}, 130 nH (see Table I), must be due largely to excess stray inductance in the measurement.

The total 3 dB bandwidth of the system, obtained by multiplication of the various poles, is slightly larger than 3 MHz. Since the bandwidth for multiplexing, defined by the on-and-off switching of first-stage SQUIDs, doesn't depend on the pole of the input circuit, the bandwidth for multiplexing will be slightly larger than the system bandwidth.

C. White noise

The contribution of the SQUID noise itself could be as low as[12]

$$\sqrt{S_{\Phi \mathrm{SQ}}} = \sqrt{18 k_B T L^2 / R_{\mathrm{sh}}} \approx 0.3 \;\; \mu\Phi_0 / \sqrt{\mathrm{Hz}}. \tag{5}$$

Other sources of noise in the system are intracoil damping resistors on the input and feedback coils of SQ1 and SQ2 as well as on the transformer coils, and the 32 address resistors of 1 Ω each in the first stage. The noise of the intracoil damping resistors is given by[10]

$$\sqrt{S_{\Phi I-C}} = \sqrt{\frac{4 k_B T n}{R_{\mathrm{ic}}}} M_1, \tag{6}$$

with n the number of coil turns, R_{ic} the intracoil damping resistance per turn, and M_1 the mutual inductance of one turn of the coil to the SQUID. $R_{\mathrm{ic}} = 30\,\mathrm{m}\Omega$ per turn for the SQ1 and SQ2 input and feedback coils. The noise of the intracoil resistors on the input and feedback coils of SQ2 is reduced due to screening by the common transformer loop. In the case of good coupling between feedback and input coil, the screening equals $(1 - L_{\mathrm{IN2}}/L_{\mathrm{TL}}) = 0.66$. All calculated values are summarized in Table III.

To transfer the second-stage noise contributions to the input of the first stage the values given in the third column of

TABLE II. Pole frequencies (MHz) for the first two stages of the MUX.

	Intracoil damping, first-stage SQUID	Bias circuit, first-stage SQUID	Intracoil damping, second-stage SQUID	Bias circuit, second-stage SQUID
Fitted to data	4.4 or 5.6	5.6 or 4.4	5.3	8.0
Calculated	4.4	4.2–4.4	5.3	6.3–11.7

Downloaded 14 Oct 2003 to 142.103.234.76. Redistribution subject to AIP license or copyright, see http://ojps.aip.org/rsio/rsicr.jsp

TABLE III. Calculated MUX noise sources at 4 K.

Contributing item	First-stage noise ($\mu\Phi_0/\sqrt{\text{Hz}}$)	Second-stage noise ($\mu\Phi_0/\sqrt{\text{Hz}}$)
SQUID noise	0.3	0.3
SQUID intracoil damping resistors	2.31 (1.85)	1.25 (0.96)
Address resistors	N.A.	0.81
Transformer intracoil damping resistors	N.A.	0.25
Total	2.33 (1.87)	1.54 (1.32)

Table III have to be divided by the first-to-second stage gain, which equals 1.0 ± 0.1. The total calculated noise for both stages transferred to the input of the first-stage is equal to $2.79\pm0.09\ \mu\Phi_0/\sqrt{\text{Hz}}$.

White-noise levels have been measured with a spectrum analyzer. Measurements were performed at several stages of the MUX, while operating subsequently the various stages in FLL mode. The measured noise levels given in Table IV are tabulated for FLL operation at a particular stage. The contribution of the third-stage noise and preamplifier noise to the previous stages of the MUX can be neglected. The measured first-stage noise is, however, clearly affected by the noise at the second stage.

Two different noise levels are measured for various SQ1s on and the second-stage in FLL, because the SQ1s are biased alternately on the positive and negative slopes of their $I-\Phi$ curve, an unintentional feature of the present design.

Given the data summarized in Table IV and the knowledge of I_Φ (Table I) for the first-stage SQUIDs, we can extract the white-noise levels for the different SQUID stages from the measurements. The first-stage noise level derived equals $1.87\pm0.10\ \mu\Phi_0/\sqrt{\text{Hz}}$, while the measured noise for the second stage equals $1.30\ \mu\Phi_0/\sqrt{\text{Hz}}$.

Both levels are significant smaller than the calculated values given in Table III. The discrepancy can be resolved by simply fitting the data, which gives an effective intra-coil resistor of 47 mΩ/turn instead of the assumed 30 mΩ/turn. The resulting calculated noise levels, now in agreement with the measurements, are given between parentheses in Table III. The higher resistance cannot be attributed to the sheet resistance of the film forming the intra-coil damping resistors, since the measurement of an on-wafer test structure confirms the intra-coil resistance of 30 mΩ.

Cooling to 100 mK should reduces the non-SQUID Johnson noise contributions to $0.35\ \mu\Phi_0/\sqrt{\text{Hz}}$. Based on experience so far with cooling individual SQUIDs the total MUX noise is expected to become $\approx 0.5\ \mu\Phi_0/\sqrt{\text{Hz}}$ at 100 mK. Initial noise measurements at 180 mK give a noise level of $0.70\ \mu\Phi_0/\sqrt{\text{Hz}}$.

TABLE IV. Measured MUX white-noise levels.

SQUIDs switched on	First stage (SQ1) in FLL	Second stage (SQ2) in FLL	Third stage (SA) in FLL
SA			$0.1\ \mu\Phi_0/\sqrt{\text{Hz}}$
SA+SQ2		$1.30\ \mu\Phi_0/\sqrt{\text{Hz}}$	
SA+SQ2+SQ1_1	$2.37\ \mu\Phi_0/\sqrt{\text{Hz}}$	$2.17\ \mu\Phi_0/\sqrt{\text{Hz}}$	
SA+SQ2+SQ1_2		$2.58\ \mu\Phi_0/\sqrt{\text{Hz}}$	

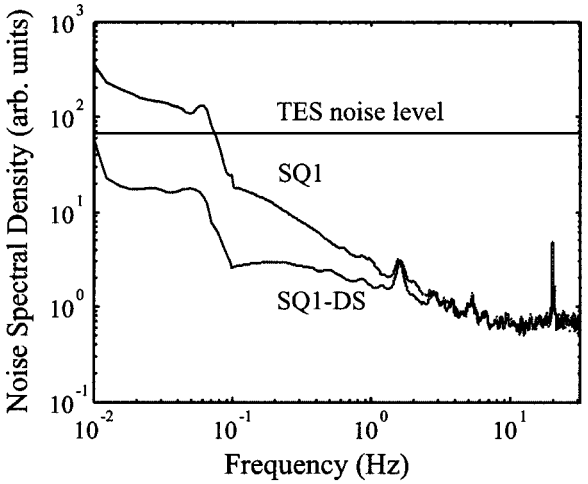

FIG. 6. Low-frequency noise spectra density of the MUX as derived from the multiplexed data set shown in Fig. 7. Both the spectra before and after ''dark'' SQUID correction are shown. Also shown is the calculated detector noise spectral density matched to the MUX noise for multiplexing 32 channels.

D. Low-frequency noise

A typical low-frequency noise spectrum for the MUX measured in the experimental setup described above is shown in Fig. 6. The corner frequency of the excess noise is about 10 Hz, and the noise spectral density of the low-frequency part scales closer to $1/f^2$ than $1/f$. The measured low-frequency spectrum cannot be accounted for by the low-frequency noise of the SQUIDs themselves, as confirmed by separate measurements on similar SQUIDs in a well-shielded, low-noise setup. So the measured low-frequency noise is caused primarily by system aspects, such as thermoelectric voltages, electromagnetic interference from external sources, bias source instability, electronics instability and harness instability, which can be largely eliminated by a careful system design.

An active technique for the reduction of a major part of the low-frequency system noise is chopping. MUX system $1/f$ noise could be eliminated by square-wave chopping the TES bias between positive and negative values. Another way of chopping is by reading a ''dark'' first-stage SQUID in every multiplex cycle of N rows. A ''dark'' SQUID (DS) is a first-stage SQUID not connected to a detector. In Fig. 7 the impact of this method on multiplexed data is shown. In this case, the noise data of only two first-stage SQUIDs are read out by means of multiplexing. The low-pass filtered signal of the DS is used to correct the data of the other SQUID. This differencing method should remove low-frequency common-mode noise in the two channels, including noise added after the signals are multiplexed together. As a result, the low-frequency noise and discrete disturbances in the corrected SQ1 are reduced. The noise spectral density of the corrected data (see Fig. 6) still has a corner frequency of 10 Hz, as for the uncorrected data, but the noise spectral density spectrum now scales as $1/f$.

Downloaded 14 Oct 2003 to 142.103.234.76. Redistribution subject to AIP license or copyright, see http://ojps.aip.org/rsio/rsicr.jsp

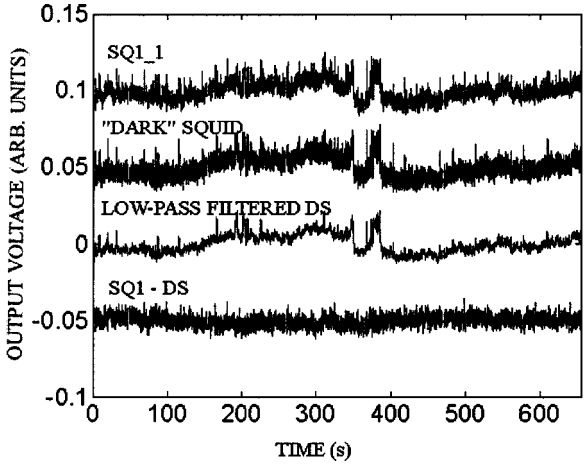

FIG. 7. Multiplexed noise data for two first-stage SQUIDs over a time period of about 600s. Also an average of the ''dark'' SQUID signal obtained by low-pass filtering is shown. The bottom curve shows data corrected by this average. A large fraction of the low-frequency noise and several specific disturbances are removed.

For 32-channel multiplexing, the noise spectral density level of the TES sensor has to be a factor 32β above the white-noise input level of the MUX.[1] Using $\beta>3$ ensures that the noise of the read out electronics is insignificant compared to the TES noise. The TES noise level is adjusted to the MUX noise level by design of the mutual inductance of the input coil and the bias resistance of the TES. The designed TES noise spectral density level is shown in Fig. 6. For this particular case, the frequencies at which the sensor white noise and MUX low-frequency noise are equal changes from 0.08 to $\approx$0.01 Hz when making use of the dark SQUID chopping technique. This is particularly important for long uninterrupted observations of the submillimeter/far-infrared sky. We believe that with careful optimization of the system the low-frequency excess noise can be reduced by this technique until it becomes limited only by the first-stage SQUID noise.

E. Multiplex bandwidth and cross talk

For several stages of the MUX, the small-signal step response has been measured in order to estimate settling times in the system. The measured time constants are in general consistent with the bandwidth measurements. The step response time τ for a signal at the input and feedback coil of SQ1 is about 50–60 ns. So, settling times for switching the FLL feedback level during multiplexing are governed by that time constant.

In addition to switching the FLL levels, multiplexing involves the successive on-and-off switching of first-stage SQUIDs. The measured time constant for that switching process is about $\tau_{\text{rise}}=60$ ns for switch-on and $\tau_{\text{fall}}=90$ ns for switch-off. The switch-on time is consistent with the measured bandwidth of the system. The switch-off time is longer, because as soon as the first stage SQUID becomes superconducting, the characteristic L/R time constant of the SQ1 bias circuit decreases from 4.3 to 2.0 MHz.

Switching one SQUID off and the subsequent one on at exactly the same time creates an output voltage overshoot at the start of each sampling period. This level is consistent with the output voltage difference between the first stage SQUID in an on and off state, and the fact that the time constants for on-and-off switching are different. The peak output voltage is equivalent to a $0.1\,\Phi_0$ signal at the first-stage input with a 60 ns rise time and 90 ns fall time. Although timing offsets between on-and-off switching of subsequent SQUIDs do significantly change this overshoot, the sampling conditions do not seem to improve.

At the start of each sample period, the output signal is allowed to settle for a fixed period of time τ_{settle} before data acquisition. Data acquisition occurs during the remaining portion of the dwell time, τ_{dwell}. If the settling time is made longer, the forward-nearest-neighbor cross talk is reduced, but the noise bandwidth of the sample is increased. If the system is run open loop, the fraction of forward-nearest-neighbor cross talk is

$$\frac{\int_{\tau_{\text{settle}}}^{\tau_{\text{dwell}}} e^{-t/\tau_{\text{fall}}} dt}{\int_{\tau_{\text{settle}}}^{\tau_{\text{dwell}}} (1-e^{-t/\tau_{\text{rise}}}) dt}. \tag{7}$$

Applying feedback significantly reduces crosstalk from the value in Eq. (7) within the feedback bandwidth, but not at higher frequencies. Thus, Eq. (7) places an upper limit on the cross talk. Different applications can tolerate different amounts of nearest-neighbor cross talk. In far-infrared bolometer systems, nearest-neighbor optical cross talk can be well above 10%. However, for x-ray spectrometers, the requirements can be much more stringent. As an example, if the system is run at a line rate of 1 MSa/s ($\tau_{\text{dwell}}=1\ \mu$s), a settle time of 600 ns is required to reduce the high-frequency forward-nearest-neighbor cross talk to below -70 dB. Cross talk to distant pixels due to this effect is much smaller.

TABLE V. Cross-talk levels.

Item	Attenuation (dB) with respect to signal input			
From SQ1 inputs to SQ2 [SQ1s off]	SQ1_1 -52 dB	SQ1_2 -61 dB	SQ1_3 -74 dB	SQ1_4 -77 dB
From SQ1 neighbors to first stage on-SQUID	Nearest-neighbor -52 dB	Next-nearest-neighbor -72 dB		
From each SQ1 to all other SQ1s by common feedback	-70 dB			

Downloaded 14 Oct 2003 to 142.103.234.76. Redistribution subject to AIP license or copyright, see http://ojps.aip.org/rsio/rsicr.jsp

In addition to the cross-talk mechanism discussed above, several other sources of cross talk have been assessed and the measured levels are summarized in Table V. One source of cross talk is that input signals to first-stage off-SQUIDs generate a small output. This cross-talk source is strongest for SQ1_1 and becomes successively smaller for successive first-stage SQUIDs. This cross talk is due to inductive coupling between the input coils of the first-stage SQUIDs and the input coil of SQ2. Another source of cross talk takes place between first-stage input signals and a neighboring on-SQUID. We give the levels for the nearest neighbor and the next-nearest neighbor of an active first-stage SQUID in Table V. All of these cross-talk sources could be reduced by modifying the geometry of the multiplexer (e.g., by increasing the spacing between adjacent inductors).

Finally, there is cross talk between a signal in each pixel of the MUX to all the other pixels in one column due to the coupling between the common feedback line and the first-stage inputs. The FLL feedback signal to each first-stage on-SQUID will be seen by all the other pixels through this coupling mechanism. The balanced SQUID pair at each input, equipped with counterwound feedback coils, as discussed before, should largely reduce this effect. Measurements show that the effective coupling $k_{\text{FB-IN}}$ between the feedback and input coil equals 1.6×10^{-2}, considerably less than in the first-generation MUX ($k_{\text{FB-IN}}\approx0.6$). The cross talk $\Delta\Phi_{\text{CT}}$ induced in all pixels connected to the common feedback line by the FLL action on a signal $\Delta\Phi_S$ in a certain pixel equals

$$\Delta\Phi_{\text{CT}}/\Delta\Phi_S = k_{\text{FB-IN}}(1-e^{-\tau_{\text{DWELL}}/\tau_{\text{IN}}})e^{-t/\tau_{\text{IN}}}, \tag{8}$$

with τ_{dwell} the dwell time at one pixel and τ_{IN} the effective time constant of the SQUID input and TES sensor bias circuit. Using the sampling frequency relation of Chervenak,[1] one finds that $\tau_{\text{DWELL}}/\tau_{\text{IN}} > \pi/\gamma N$ with $\gamma>3$ and N the number of pixels multiplexed in one column. If we take $t=\frac{1}{2}N\tau_{\text{DWELL}}$ and $N=32$ this cross talk is -70 dB, acceptable for most applications presently foreseen. Another effect of the coupling between feedback and input is that each sensor gets a power input equal to $(k_{\text{FB-IN}})^2/N$ of the signal power in any other of the $N-1$ pixels. For $N=32$ this equals -100 dB.

The coupling of the bias line to the input coil of the first-stage on-SQUID is not balanced, since the bias line to the dummy SQUID is not connected. Therefore, the switch-on of a SQUID generates screening currents in the input circuit equivalent to about 0.1 Φ_0 for the present configuration. Since the time constant of the input circuit coupled to a TES is much longer then the dwell time this results in an offset for each pixel. As long as this offset is constant it is of little concern, and it should be possible to eliminate this effect in future designs.

F. Multiplex examples

The functionality of our SQUID MUX has been tested using a digital FLL feedback[13] (DFB) scheme, the characteristics of which will be discussed in a separate article. In short, the DFB works as follows. During the dwell time τ_{DWELL} of a first-stage SQUID the MUX output signal is sampled, digitized and averaged. The averaged signal is used to calculate a feedback signal by means of a PI algorithm. This feedback signal is applied to the common first-stage feedback line FB1 at the subsequent dwell time of the first stage SQUID readout, i.e., the feedback to a particular first-stage SQUID takes place at the frame rate $1/\tau_{\text{FRAME}}=1/N\tau_{\text{DWELL}}$, which is a direct measure of the feedback bandwidth. As an example, sine-wave currents with frequencies of 300 Hz–2.4 kHz and peak-to-peak amplitudes corresponding to 2 Φ_0 in the first-stage SQUIDs were applied to eight different input stages of the 32-channel multiplexer. A dwell time $\tau_{\text{DWELL}}=1.28\,\mu$s was chosen. The demultiplexed signals of the 8 SQUID MUX channels are shown in Fig. 8.

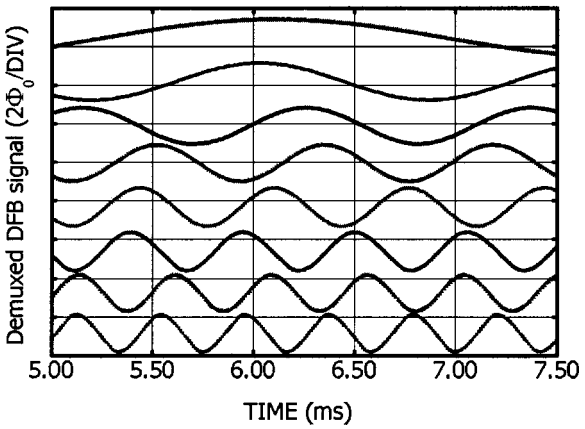

FIG. 8. Functionality test of the SQUID MUX with digital feedback. Sine-wave currents with frequencies of 300 Hz–2.4 kHz and peak-to-peak amplitudes corresponding to 2 Φ_0 in the first-stage SQUIDs were applied to eight input coils. The dwell time τ_{DWELL} was 1.28 μs per channel. The demultiplexed feedback signals are shown. The curves are vertically shifted for clarity.

V. SUMMARY AND RECOMMENDATIONS

A second-generation TDM for 32 channels has been designed, fabricated, and tested. The system has a bandwidth of approximately 3 MHz, and multiplexing of eight channels in digital FLL up to a sample rate of 0.78 MSa/s has been demonstrated. The system noise level at the input of the first stage will be very close to $0.5\,\mu\Phi_0/\sqrt{\text{Hz}}$ at 100 mK. The system is well suited for forthcoming submillimeter/far-infrared imaging bolometer arrays, such as SCUBA-2, as well as for x-ray microcalorimeter arrays, such as the one for Constellation X.

Relatively small improvements considered for future designs are (1) the reduction of the cross talk between the first and second stage by increase of the distance between SQ2 and the first-stage input SQUIDs, and (2) suppression of the coupling between the bias line of each first-stage SQUID to its input circuit by the implementation of a symmetrical bias design.

More important, especially for x-ray microcalorimeter applications, is the increase of bandwidth. Within the present architecture the bandwidth can be improved by a number of measures. Increase of the intracoil damping resistors on all SQUIDs by a factor of 4, almost certainly possible without any penalty in SQUID-coil resonances, will move the poles

Downloaded 14 Oct 2003 to 142.103.234.76. Redistribution subject to AIP license or copyright, see http://ojps.aip.org/rsio/rsicr.jsp

caused by the coil self inductances and the coil damping resistors above 20 MHz. Modifications of the connections to the present series-array SQUID will enable reduction of the input inductance by about a factor 2, moving the pole due to the dynamic resistance of SQ2 and the input self-inductance of the SA to 15 MHz. Further increase in the bandwidth of the coupling to the series-array SQUID could be made by modification of the series-array design, for example the introduction of a step-up transformer on the series-array input, while increasing the number of turns per SQUID, or reduction of the number of SQUIDs in the series array while increasing the number of turns. In order to increase the bandwidth of the bias circuit of SQ1, presently 4.4 to 5.6 MHz, the inductance L_{TL} of the transformer loop can be reduced. The transfer from SQ1 to SQ2 is given by Eq. (1). So, reduction of L_{TL} allows for reduction of M_{INT}, and resulting also in the required reduction of L_{INT}, thereby increasing the bandwidth of the bias circuit. Reduction of L_{TL} can be obtained in two ways: (1) reduction of the stray components by use of wider strip lines in the transformer secondary coil and (2) reduction of L_{IN2} by use of a standard, nonfloating, washer SQUID with high coupling efficiency. Both measures will reduce L_{TL} by about a factor of 2, so that M_{INT} can be decreased by a factor of 2 as well, increasing the bandwidth by a factor of 4. This is achieved by changing the transformer coils turns ratio to 10:1, so that L_{INT} would become approximately 20 nH, resulting in a bandwidth of 21 MHz.

In summary, we expect that the bandwidths of all poles in the SQUID multiplexing circuit could be increased to about 20 MHz, increasing the achievable sample rate by about a factor of 4 to approximately 12 MHz. Further increase in the bandwidth would likely require a modification of the circuit architecture.

Some scope also exists to reduce the input system noise. Enhancement of gain between the first and second stage could reduce the noise to about 0.4 $\mu\Phi_0/\sqrt{\mathrm{Hz}}$ at 100 mK. Reduction of the intracoil damping resistors as envisaged for the bandwidth might bring the noise down further.

ACKNOWLEDGMENTS

This work was supported in part by NASA under Contract Nos. S-94800-Y and S-03970-G. Contribution of an agency of the U.S. Government; not subject to copyright.

[1] J. A. Chervenak, K. D. Irwin, E. N. Grossman, J. M. Martinis, C. D. Reintsema, and M. E. Huber, Appl. Phys. Lett. **74**, 4043 (1999).
[2] J. Yoon, Appl. Phys. Lett. **78**, 371 (2001).
[3] K. D. Irwin, Physica C **368**, 203 (2002).
[4] M. Kiviranta, H. Seppae, J. van der Kuur, and P. de Korte, AIP Conf. Proc. **605**, 295 (2002).
[5] D. J. Benford *et al.*, Int. J. Infrared Millim. Waves **21**, 1909 (2000).
[6] D. J. Benford *et al.*, AIP Conf. Proc. **605**, 589 (2002).
[7] K. D. Irwin, L. R. Vale, N. E. Bergren, S. Deiker, E. N. Grossman, G. C. Hilton, S. W. Nam, C. D. Reintsema, D. A. Rudman, and M. E. Huber, AIP Conf. Proc. **605**, 301 (2002).
[8] J. E. Sauvageau, C. J. Burroughs, P. A. A. Booi, M. W. Cromar, S. P. Benz, and J. A. Koch, IEEE Trans. Appl. Supercond. **5**, 2303 (1995).
[9] M. E. Huber, P. A. Neil, R. G. Benson, D. A. Burns, A. M. Corey, C. S. Flynn, Y. Kitaygorodskaya, O. Massihzadeh, J. M. Martinis, and G. C. Hilton, IEEE Trans. Appl. Supercond. **11**, 1251 (2000).
[10] M. E. Huber, A. H. Steinbach, and R. H. Ono, Physica C **351**, 85 (2001).
[11] J. M. Jaycox and M. B. Ketchen, IEEE Trans. Magn. **17**, 400 (1981).
[12] John Clarke, Proc. IEEE **77**, 1208 (1989).
[13] J. A. Chervenak, E. N. Grossman, K. D. Irwin, J. M. Martinis, C. D. Reintsema, C. A. Allen, D. I. Bergman, S. H. Moseley, and R. Shafer, AIP Conf. Proc. **605**, 107 (2002).

Downloaded 14 Oct 2003 to 142.103.234.76. Redistribution subject to AIP license or copyright, see http://ojps.aip.org/rsio/rsicr.jsp